The Journal of Immunology

Molecular Requirements for MHC Class II α -Chain Engagement and Allelic Discrimination by the Bacterial Superantigen Streptococcal Pyrogenic Exotoxin C

Katherine J. Kasper, Wang Xi, A. K. M. Nur-ur Rahman, Mohammed M. Nooh, Malak Kotb, Eric J. Sundberg, Joaquín Madrenas and John K. McCormick

J Immunol 2008; 181:3384-3392; ;
doi: 10.4049/jimmunol.181.5.3384
http://www.jimmunol.org/content/181/5/3384

The Journal of Immunology is published twice each month by
The American Association of Immunologists, Inc.,
1451 Rockville Pike, Suite 650, Rockville, MD 20852

Print ISSN: 0022-1767 Online ISSN: 1550-6606.

Molecular Requirements for MHC Class II α-Chain Engagement and Allelic Discrimination by the Bacterial Superantigen Streptococcal Pyrogenic Exotoxin C[1]

Katherine J. Kasper,*† Wang Xi,*‡ A. K. M. Nur-ur Rahman,*† Mohammed M. Nooh,§ Malak Kotb,§¶ Eric J. Sundberg,‖ Joaquín Madrenas,*‡ and John K. McCormick[2]*†

Superantigens (SAgs) are microbial toxins that bind to both TCR β-chain variable domains (Vβs) and MHC class II molecules, resulting in the activation of T cells in a Vβ-specific manner. It is now well established that different isoforms of MHC II molecules can play a significant role in the immune response to bacterial SAgs. In this work, using directed mutational studies in conjunction with functional analyses, we provide a complete functional map of the low-affinity MHC II α-chain binding interface of the SAg streptococcal pyrogenic exotoxin C (SpeC) and identify a functional epitope in the β-barrel domain that is required for the activation of T cells. Using cell lines that exclusively express individual MHC II isoforms, our studies provide a molecular basis for the selectivity of SpeC-MHC II recognition, and provide one mechanism by how SAgs are capable of distinguishing between different MHC II alleles. ***The Journal of Immunology,*** **2008, 181: 3384–3392.**

Superantigens (SAgs)[3] are microbial toxins that function to simultaneously engage the lateral surfaces of MHC class II molecules (1–8) and TCR β-chain variable regions (Vβs) (9–15). The unconventional contacts that SAgs make with these two adaptive immune receptors allows for the activation of large numbers of T cells that initially expand in a Vβ-specific manner (16). In severe cases of SAg exposure the ensuing cytokine "storm" can result in the toxic shock syndrome (17, 18), and SAgs have also been implicated in a variety of other immune-mediated diseases (19–22). Despite engagement of MHC II as one defining feature of SAgs and a wealth of structural information regarding how SAgs bind MHC II, there is generally little data to indicate the molecular requirements for MHC II discrimination.

*Department of Microbiology and Immunology, University of Western Ontario, †Lawson Health Research Institute, ‡Federation of Clinical Immunology Societies (FOCIS) Centre for Clinical Immunology and Immunotherapeutics, and Robarts Research Institute, London, Ontario, Canada; §Department of Research Service, Veterans Affairs Medical Center, Mid-South Center for Biodefense and Security, University of Tennessee Health Science Center, Memphis, TN 38163; ¶Department of Molecular Genetics, Biochemistry and Microbiology, University of Cincinnati, Cincinnati, OH 45627; and ‖Boston Biomedical Research Institute, Watertown, MA 02472

Received for publication May 2, 2008. Accepted for publication June 26, 2008.

The costs of publication of this article were defrayed in part by the payment of page charges. This article must therefore be hereby marked *advertisement* in accordance with 18 U.S.C. Section 1734 solely to indicate this fact.

[1] This work was supported by Canadian Institutes of Health Research (CIHR) operating grants to J.K.M. and J.M. and National Institutes of Health Grant AI55882 to E.J.S. Stipend support to K.K. and A.K.M.N.R. was provided in part by scholarships from the Schulich School of Medicine and Dentistry and by an Early Research Award from The Ontario Ministry of Research and Innovation. Laboratory infrastructure was supported by a New Opportunities Fund award from the Canadian Foundation for Innovation and the Ontario Innovation Trust (to J.K.M). J.M. holds a Tier I Canada Research Chair in Immunobiology, and J.K.M. holds a New Investigator award from CIHR.

[2] Address correspondence and reprint requests to Dr. John K. McCormick, Department of Microbiology and Immunology, University of Western Ontario, London, Ontario, Canada N6A 5C1. E-mail address: john.mccormick@schulich.uwo.ca

[3] Abbreviations used in this paper: SAg, superantigen; BLS, bare lymphocyte syndrome; MHCα, MHC II α-chain; MHCβ, MHC II β-chain; SE, staphylococcal enterotoxin; SEA/SEB/SEC_3/SEE, staphylococcal exotoxin A, B, C_3, or E; SpeA/SpeC, streptococcal pyrogenic exotoxin A or C; SSA, streptococcal superantigen; TEV, tobacco etch virus; TSST-1, toxic shock syndrome toxin-1; Vβ, variable region of the TCR β-chain.

Bacterial genome sequencing projects have revealed that there are a large number of genetically distinct SAgs, of which there are >30 identified serotypes (23), that can be classified into at least five distinct evolutionary groups (I–V) (18, 24, 25). A phylogenetic tree showing this classification scheme has been recently published (24). Pyrogenic toxin SAgs include the toxic shock syndrome toxin-1 (TSST-1) and numerous staphylococcal enterotoxin serotypes produced by *Staphylococcus aureus*, as well as multiple streptococcal pyrogenic exotoxin serotypes produced by *Streptococcus pyogenes* and related β-hemolytic streptococci (18). Although these toxins all have a generally conserved structure including an N-terminal β-barrel domain and a larger C-terminal β-grasp domain (26), each distinct evolutionary group likely engages host receptors in structurally and functionally distinct ways.

The TCR Vβ binding interface on the surface of SAgs exists in a relatively conserved position located in a groove between the β-barrel domain and the β-grasp domain and invariably involves the SAg N-terminal α-helix. However, each characterized SAg evolutionary group demonstrates unique TCR Vβ binding contacts and orientations and, thus, each group results in altered T cell activation complexes (25).

Engagement of MHC II by SAgs is more variable than Vβ engagement and can occur through at least three clearly distinct modes. For example, TSST-1 (the only group I SAg) binds the MHC II α-chain (MHCα) through the TSST-1 N-terminal β-barrel domain in a relatively low-affinity ($K_D \sim 10^{-5}$) interaction that also engages the antigenic peptide and makes contacts within the β1 domain of the MHC II β-chain (MHCβ) (3) (Fig. 1). Thus, TSST-1 engagement of MHC II can be strongly influenced by the antigenic peptide (27). Group II SAgs such as staphylococcal enterotoxin B (SEB) and staphylococcal enterotoxin C_3 (SEC_3), as well as the group III SAg staphylococcal enterotoxin A (SEA), each engage MHCα similarly, although these toxins bind to a more lateral region on MHCα compared with TSST-1 and, consequently, these interactions are peptide independent (2, 4, 8) (Fig. 1). Currently, there is no structural data to indicate how the group IV or the group V SAg engages MHCα. In addition to the low-affinity MHCα binding, group III (7), group IV (6), and group V (5) SAgs are known to bind MHCβ in an essentially conserved,

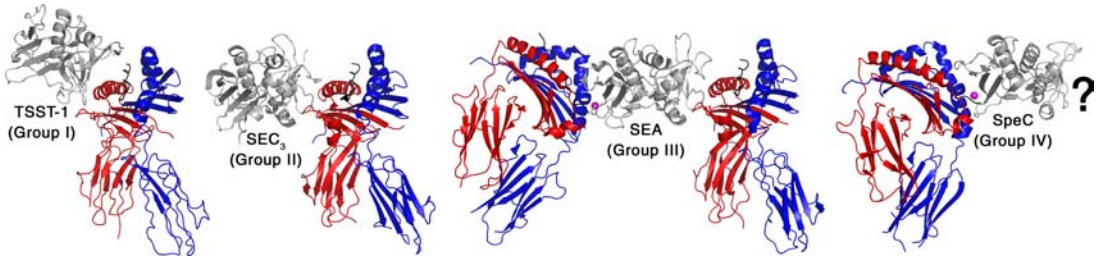

FIGURE 1. Structural overview of bacterial SAgs from the various evolutionary groups (I, II, III, and IV) in complex with MHC II. Individual SAgs are labeled and colored gray, MHCα-chains are colored red, MHCβ-chains are colored blue, antigenic peptides are colored black, and zinc atoms are colored magenta. Ribbon diagrams were generated using PyMOL (pymol.sourceforge.net/) from the crystal structures of TSST-1 (3), SEC_3 (4), SEA_{D227A} (8), SEH (7), and SpeC (6) in complex with MHC II. As previously described (8), the ternary model of SEA-$(MHC)_2$ was produced by superimposing the low-affinity HLA-DR1-SEA_{D227A} complex with the high-affinity HLA-DR1-SEH complex to orient the high-affinity MHC II interaction with SEA. The "question mark" indicates the uncharacterized MHC II interaction with SpeC analyzed in this study.

relatively high-affinity ($K_D \sim 10^{-7}$ M) zinc-dependent manner that occurs through the β-barrel domain located on the opposing face of the SAg (Fig. 1). The high-affinity MHCβ interaction acts by coordinating a zinc ion with three conserved SAg amino acids, and the zinc ion is also coordinated by a conserved amino acid on the polymorphic β-chain (βHis^{81}). Mutations in any of the four residues that coordinate zinc severely disrupt the activity of the SAg (28–34). Although MHCβ is highly polymorphic and much of the buried surface with the MHC β-chain is mediated by the antigenic peptide, this binding arrangement targets conservatively substituted MHCβ residues and engages the N terminus of the peptide, which is also conformationally conserved (5). Some SAgs such as SEA have been shown to cross-link MHC II molecules by binding to both MHCα and MHCβ (28, 35, 36) (Fig. 1).

It is now well established that MHC II discrimination by SAgs can play a profound role in both the magnitude of the immune response and the clinical outcome of severe invasive streptococcal infections (37–44). However, the molecular basis by which a particular SAg binds preferentially to certain MHC II molecules but poorly recognizes others is not well understood. To understand why SAgs preferentially engage certain MHC II molecules and to further understand receptor engagement by the group IV SAgs, we have mutated the molecular surface of streptococcal pyrogenic exotoxin C (SpeC) predicted to engage MHCα. Our findings provide the "functional epitope" on the SpeC molecular surface for engagement of different MHCα isoforms and, based on modeled complexes, we provide a molecular basis for SpeC-MHC II discrimination.

Materials and Methods

Cloning procedures

Standard DNA manipulations were performed as described (45) using enzymes supplied from New England Biolabs in accordance with the manufacturer's instructions. Oligonucleotides were obtained from Invitrogen. PCRs were performed in a Peltier thermocycler (MJ Research) with *Vent* DNA polymerase (Invitrogen), and PCR products were purified using the QIAquick PCR purification kit (Qiagen). All cloned PCR products were sequenced in their entirety at the John P. Robarts Research Institute Sequencing Facility (London, Ontario, Canada) to ensure correct mutations and PCR fidelity. *Escherichia coli* was cultured aerobically in Luria Bertani broth (Difco) at 37°C, and solid medium was obtained by the addition of 1.5% (w/v) Bacto agar (Difco). Kanamycin (50 μg/ml) was used as a selective agent as required. All reagents were made with water purified through a Milli-Q water purification system (Millipore).

SpeC Mutants

Cloning and expression of the various SpeC proteins (46–48) were performed using the modified *E. coli* expression vector pET41a::TEV, where the pET41a (Novagen) enterokinase cleavage site (DDDDK) is replaced with the tobacco etch virus (TEV) protease cleavage site (ENLYFQG) (49). Each SpeC mutant was generated using an overlapping megaprimer PCR method with oligonucleotides that incorporated the desired single-site mutation. SpeC proteins were expressed from *E. coli* BL21 (DE3) (Novagen) purified by Ni^{2+} column chromatography, and the purification tags were removed with autoinactivation-resistant His7::TEV as described (50). All SpeC proteins were purified to apparent homogeneity as determined by SDS-PAGE (data not shown). Key mutant proteins lacking functional activity were examined by circular dichroism analysis to confirm that the point mutations did not induce any gross structural deviations in the proteins (data not shown).

LG-2 aggregation assay

The B lymphoid cell line LG-2 was used in cell aggregation experiments (46) where the cells (100,000/ml) were suspended in R10 medium (RPMI 1640 (Invitrogen) supplemented with 10% FCS (Sigma-Aldrich), 100 μg/ml streptomycin (HyClone), 100 U/ml penicillin (HyClone), 2 mM L-glutamine (HyClone), 1 mM MEM sodium pyruvate (HyClone), 100 μM nonessential amino acid (HyClone), and 25 mM HEPES (pH 7.2) (BioShop)) and plated into each well of a 96-well plate. Afterward, each SpeC protein (1 μg/ml) was added and aggregation was monitored using an inverted microscope at various time points. The reversibility of the high-affinity MHC II binding site (51) was tested by the addition of 1 mM EDTA after 2 h to chelate divalent cations and then by the addition of 2 mM $ZnSO_4$ after 4 h. Results were assessed as the number of cells in clumps as a percentage of the total number of cells in the field of view at $\times$100 original magnification.

Functional mapping of the MHCα binding interface of SpeC using Vβ2.1$^+$ Jurkat T cells

Vβ2$^+$ T cells are the major target of SpeC (46). Thus, we used the Jurkat T cell line eJRT3-2.1 engineered to express the Vβ2.1 chain used in the SpeC-Vβ2.1 complex (13), which pairs with the endogenous TCR α1-chain variable region (Vα1). APCs included the B lymphoid cell line LG-2, which is homozygous for the expression of HLA-DR1 (DRA*0101/DRB1*0101), HLA-DQ5 (DQA1*010101/DQB*05010101) and HLA-DP3 (DPA1*010301/DPB1*0301) (52), or the type II bare lymphocyte syndrome (BLS) B cells, which exclusively express HLA-DR1 (DRA1*0101/DRB1*0101), HLA-DR4 (DRA1*0101/DRB1*0401), or HLA-DQ2α3β (DQA1*0501/DQB1*0302) (42). Activation was monitored for IL-2 production by ELISA (BD Biosciences) using eJRT3-2.1 cells incubated in the presence of SpeC proteins (1 or 100 ng/ml as indicated) for 18 h with the various APC lines. For phosphorylation of ERK-1/2, LG-2 cells were preincubated with SpeC proteins (10 ng/ml) for 30 min and eJRT3-2.1 cells were added at a 5:1 ratio with the preincubated LG-2 cells. Cells were harvested and washed with cold PBS containing sodium orthovanadate at 400 μM to inhibit tyrosine phosphatases. The cells were lysed in 1% Triton X-100 lysis buffer and analyzed by Western blotting for total ERK-1/2 using rabbit polyclonal immunoaffinity-purified antiserum (Stressgen Biotechnologies) and for active ERK-1/2 with mAb E10 (Cell Signaling Technology).

Three-dimensional models

The quaternary model of the SpeC-mediated T cell activation complex was constructed by superimposing the crystal structure of SpeC-Vβ2.1 (Protein Data Bank code 1KTK) (13) with the SEC3-HLA-DR1 complex (Protein Data Bank code 1JWM) (4) to orientate the low-affinity MHC class II

interaction. The high-affinity MHC II interaction was oriented to SpeC by superimposing the SpeC-HLA-DR2a complex (Protein Data Bank code 1HQR) (6), and the TCR α-chain was oriented from a typical TCR-MHC II interaction (Protein Data Bank code 1FYT) (53).

Statistical analysis

Bar graphs are shown as mean ± SEM and represent 3–10 separate experiments as indicated. Statistical analyses for comparing mutant proteins with the wild-type proteins were performed using one-way ANOVA with Dunnett's multiple comparison test (GraphPad Prism 4). Differences were considered significant when $p < 0.05$.

Results

Generation of the SpeC mutants

Previous work has shown that SpeC is able to aggregate the B lymphoid cell line LG-2, and that this aggregation phenotype was attributed to the ability of SpeC to form zinc-mediated homodimers that bind adjacent MHC II molecules through the high-affinity interaction present on each monomer (46). From the crystal structure of SpeC, the dimer interface occupied the generic, low-affinity MHC II domain and thus precluded the low-affinity interaction (47). However, other work using limited mutational analysis has shown that SpeC likely possesses an alternative MHC II binding interface (29, 48) analogous to the structurally characterized low-affinity interfaces of SEA, SEB and SEC_3 (2, 4, 8). Thus, to resolve the issue regarding the presence or absence of a potential low-affinity MHC II binding interface and to understand the molecular basis by which SpeC binds MHC II through this putative interface, we performed alanine-scanning mutagenesis of all SpeC residues within the β-barrel domain that could potentially contact MHC II. These mutations were initially based on the four structurally characterized SAg/low-affinity MHC II interactions including TSST-1/HLA-DR1 (3), SEB/HLA-DR1 (2), SEA_{D227A}/HLA-DR1 (8), and SEC_3/HLA-DR1 (4). A total of 20 mutations were engineered that cover 2,192 Å (2) of the SpeC surface, as well as two additional control mutations located within the characterized zinc-mediated, high-affinity MHCβ ($SpeC_{D203A}$) and TCR ($SpeC_{Y15A}$) interfaces (6, 13), each of which are known to disrupt these respective interactions (29, 49).

LG-2 cell aggregation by the SpeC mutants is indicative of multiple binding interfaces on SpeC

We first confirmed the ability of wild-type SpeC to aggregate the LG-2 B lymphoid cell line (46), which is homozygous for the expressions of HLA-DR1, HLA-DQ5, and HLA-DP2 (52). LG-2 cells aggregated upon the addition of staphylococcal enterotoxin E (SEE), a SAg containing both the high-affinity and low-affinity MHC II binding interfaces, whereas cells treated in parallel with streptococcal pyrogenic exotoxin A (SpeA), a streptococcal SAg containing only the low-affinity MHC II binding interface, did not (Fig. 2*A*). As expected (46), SpeC aggregated LG-2 cells in a similar manner to that of SEE (Fig. 2*A*). The nature of this aggregation was zinc dependent because the chelation of divalent cations by the addition of EDTA disrupted aggregation, which was reversible upon the addition of excess zinc (Fig. 2*B*). The aggregation phenotype was disrupted by an alanine point mutation in the control high-affinity interface mutant (at SpeC position Asp^{203}), while the control TCR interface mutation (at SpeC position Tyr^{15}) predictably did not disrupt the phenotype (Fig. 2*C*). Of the 20 mutations within the putative low-affinity interface, alanine substitutions at positions Tyr^{50}, Tyr^{76}, and Tyr^{87} each significantly disrupted the aggregation phenotype (Fig. 2*C*). These data suggest that there are two independent interfaces on SpeC responsible for the LG-2 cell aggregation phenotype, one that is represented by the zinc-dependent, high-affinity MHC II interface (6, 29), and a second within the β-barrel domain that is consistent with characterized low-affinity MHC II interfaces (2–4, 8).

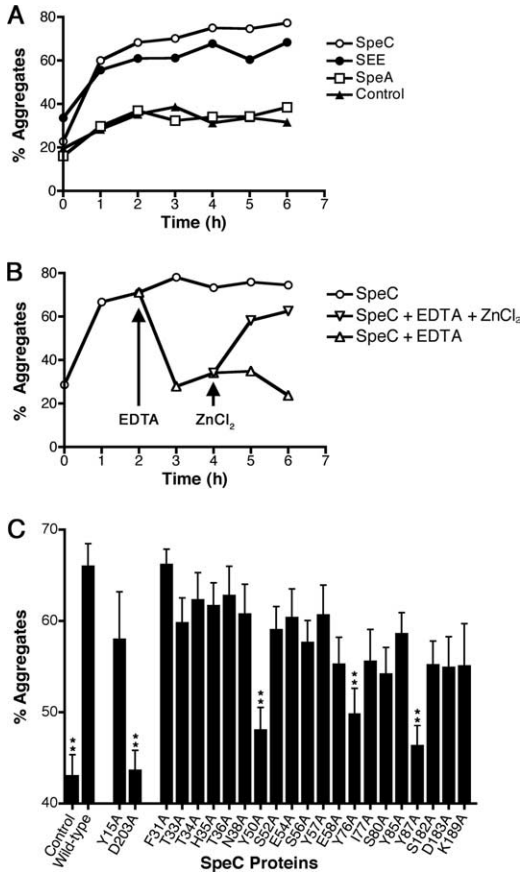

FIGURE 2. Aggregation phenotypes of the B-lymphoid cell line LG-2 cells by SpeC. LG-2 cells (100,000 cells/well) were treated with the various SAg proteins at 1 μg/ml and aggregation was assessed by light microscopy. *A*, Cells treated with SEE, known to contain both high- and low-affinity MHC II binding interfaces (28, 63), induced aggregation, whereas cells treated with SpeA, which contains only the low-affinity MHC II binding interface, did not aggregate more than cells not treated with SAg. SpeC aggregated LG-2 cells similarly as SEE. *B*, The aggregation of LG-2 cells by SpeC is zinc dependent and reversible, as the chelation of divalent cations with EDTA disrupted aggregation and the addition of $ZnCl_2$ in molar excess restored aggregation. *C*, Aggregation of LG-2 cells is disrupted by mutations in the low-affinity MHC II binding interface of SpeC. Cells were observed at the 4-h time point for multiple mutant SpeC proteins. Cells not treated with SAg were used as background control. Additional controls included cells treated with the $SpeC_{Y15A}$ mutant known to be critical for engagement of TCR (13, 49) and the $SpeC_{D203A}$ mutant known to be critical for engagement of MHCβ through the high-affinity interface (6, 29). Data shown are the average ± SEM for at least 10 independent experiments. **, $p < 0.01$.

Mutations within the putative low-affinity MHC II binding interface of SpeC impair T cell activation

Because the major targets of SpeC are T cells expressing the Vβ2 TCR (46, 49), we monitored the activation of the engineered Vβ2.1$^+$ Jurkat T cell line eJRT3-2.1 (49) in the presence of LG-2 cells by the production of IL-2 and the phosphorylation of ERK-1/2 in response to the various SpeC mutants (Fig. 3). Consistent with the LG-2 aggregation data, point mutations at Tyr^{50} and Tyr^{87} severely impaired the ability to activate T cells (Fig. 3*A*). Mutations at Tyr^{76}, Ile^{77}, and Tyr^{85} showed an intermediate decrease in activity, whereas mutations at Thr^{36} and Asp^{183} produced

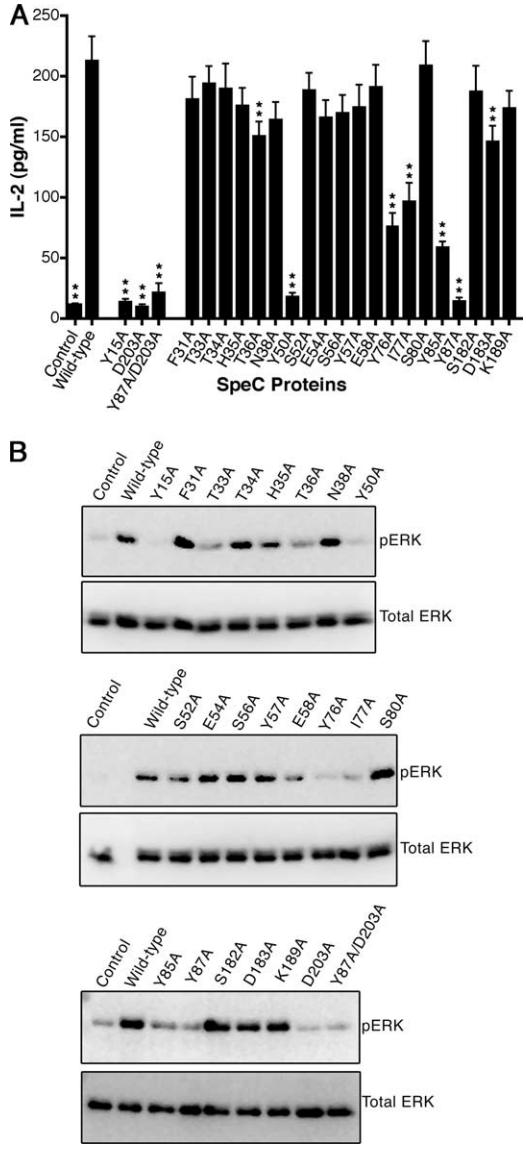

FIGURE 3. Functional analysis of the SpeC low-affinity MHC II binding interface. *A*, IL-2 secretion by eJRT3-2.1 T cells incubated with the SpeC mutant proteins at 1 ng/ml in the presence of LG-2 cells. Controls are similar to those presented in Fig. 2. Data shown are the average ± SEM for at least six independent experiments, each done in triplicate. **, $p < 0.01$ *B*, ERK-1 and ERK-2 activation by eJRT3-2.1 cells incubated with the SpeC mutant proteins at 10 ng/ml in the presence of LG-2 cells as described in *Materials and Methods*. pERK, phosphorylated ERK.

mild but significant reductions in activity. The remainder of the mutants showed little to no reductions in activity. The control mutants $SpeC_{Y15A}$ and $SpeC_{D203A}$, as well as the additional double mutant $SpeC_{Y87A/D203A}$, behaved as expected and did not produce significant quantities of IL-2.

Becauses bacterial SAgs can activate T cells through two distinct activation pathways, both of which converge upon the phosphorylation of ERK-1/2 (54), we also measured the phosphorylation of ERK-1/2 in the presence of the various mutants as a measure of SpeC-induced T cell signaling (Fig. 3*B*). Consistent with the IL-2 activation experiments, the mutant proteins $SpeC_{T36A}$, $SpeC_{Y50A}$, $SpeC_{Y76A}$, $SpeC_{I77A}$, $SpeC_{Y85A}$, and $SpeC_{Y87A}$ were impaired for the ability to activate ERK-1/2. In addition, $SpeC_{T33A}$ showed a reduced ERK-1/2 activation phenotype that was not seen with the IL-2 activation experiments. The remainder of the mutants showed little to no reductions in activity. The control mutants $SpeC_{Y15A}$ and $SpeC_{D203A}$, as well as the additional double mutant $SpeC_{Y87A/D203A}$, behaved as expected and did not activate ERK-1/2.

These data indicate that a discrete number of residues within the β-barrel domain of SpeC are important for the activation of Vβ2.1$^+$ T cells, and that these mutations likely disrupt the ability of SpeC to engage MHCα.

SpeC interacts with HLA-DR and HLA-DQ in different ways

To evaluate the ability of specific MHC II molecules to present the various SpeC mutants, we used BLS B cells transfected with specific MHC II alleles (HLA-DR1, HLA-DR4, or HLA-DQ2α3β) (42). BLS is an autosomal recessive disease in which the transcription factors that bind to MHC II promoters are mutated. As such, constitutive and inducible expression of MHC II is absent (55). Because SpeC was previously reported to activate T cells more strongly in the presence of HLA-DR4 compared with HLA-DQ2α3β (42), we first tested the activation of eJRT3-2.1 T cells with titrated SpeC in the presence of the different APC cell lines. As shown in Fig. 4*A*, SpeC activated eJRT3-2.1 T cells at ~100–1000 times lower concentration with BLS cells expressing HLA-DR4 compared with HLA-DQ2α3β. Thus, we conducted the remainder of experiments with the SpeC proteins at 1 ng/ml in the presence of HLA-DR4 or HLA-DR1 and at 100 ng/ml in the presence of HLA-DQ2α3β. The overall activation profile of the various SpeC mutants in the presence of HLA-DR4 (Fig. 4*B*) or HLA-DR1 (Fig. 4*C*), was very similar, with mutations at positions Tyr^{50}, Tyr^{76}, Ile^{77}, Tyr^{85}, Tyr^{87}, and Asp^{183} showing the most drastic phenotypes. Mutations at positions Thr^{36} demonstrated an intermediate phenotype for both HLA-DR1 and HLA-DR4, Thr^{33} was significantly reduced for HLA-DR4, and Asn^{38} was significantly reduced for HLA-DR1. The remainder of the mutations at positions Thr^{34}, His^{35}, Tyr^{57}, Glu^{58}, and Lys^{189} showed little to no effect. The $SpeC_{S80A}$ mutant demonstrated a moderate but consistent increase in activity.

The activation profile of the various SpeC mutants in the presence of HLA-DQ2α3β (Fig. 4*D*) showed an overall different pattern for the various mutations. Reductions in activity for mutations at SpeC positions Tyr^{50}, Tyr^{76}, and Tyr^{87} were common with all three MHC II molecules, whereas mutations at positions Thr^{36}, Ile^{77}, Tyr^{85}, and Asp^{183} showed reduced activity only for the HLA-DR alleles and mutations at positions Thr^{34}, His^{35}, and Glu^{54} showed reduced activity only in the presence of HLA-DQ2α3β. In all cases, the control mutants $SpeC_{Y15A}$ and $SpeC_{D203A}$, as well as the additional double mutant $SpeC_{Y87A/D203A}$, behaved as expected and did not result in significant amounts of IL-2. Collectively, these results show that SpeC uses different patterns of residues to engage the α-chains of different MHC II molecules.

Three-dimensional model of the TCR-SpeC-(MHC II)$_2$ signaling complex

A structural "map" of the various residues that were mutated in this study is summarized in Table I and shown as a ribbon diagram in Fig. 5*A*, where the side chains of relevant amino acids, including the control mutations at SpeC positions Tyr^{15} and Asp^{203}, are shown and indicated. In Fig. 5, *B* and *C*, the molecular surfaces of SpeC that were important for the engagement of HLA-DR4 and HLA-DQ2α3β, respectively, are shown. Mutated positions that produced activation profiles similar to negative control conditions and were therefore determined to be critical, are colored red. Mutated positions with an intermediate phenotype are colored yellow, and those that did not result in significantly decreased activity are colored green.

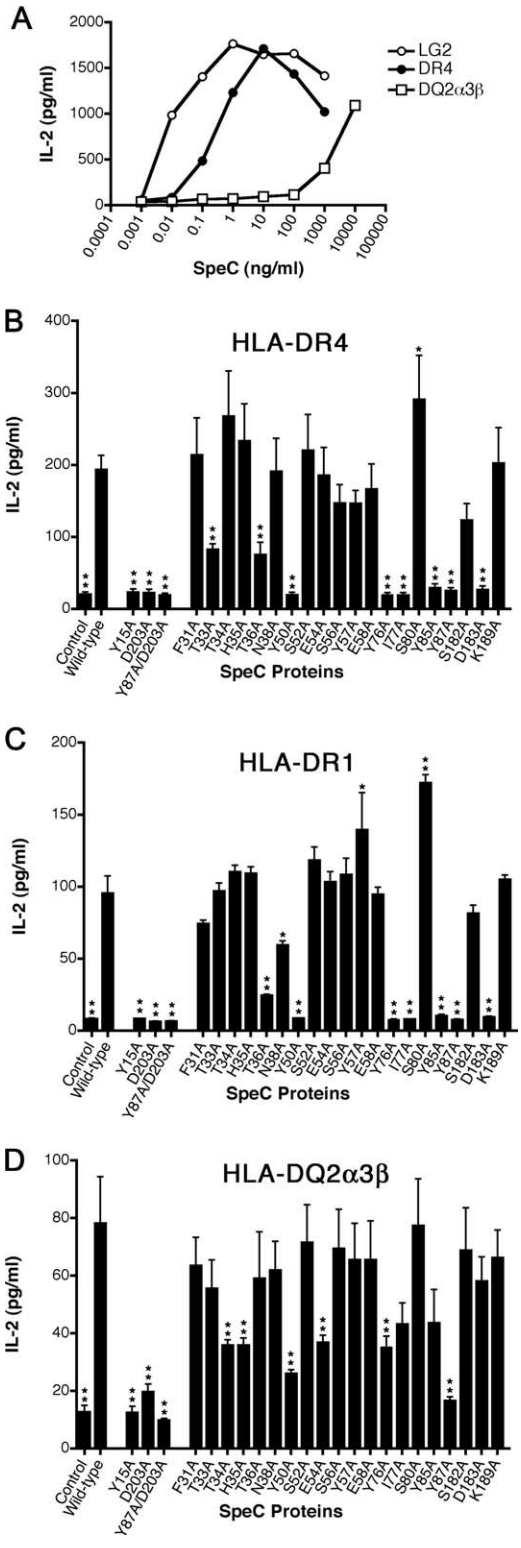

FIGURE 4. Functional analysis of the SpeC low-affinity MHC II binding interface for interaction with defined MHC haplotypes. *A*, SpeC activated eJRT3-2.1 T cells at ~100–1000 times lower concentration with BLS cells expressing HLA-DR4 (●) compared with HLA-DQ2α3β (□). *B–D*, IL-2 secretion by eJRT3-2.1 T cells incubated with the SpeC mutant proteins in the presence of BLS cells expressing HLA-DR4 (*B*), HLA-DR1 (*C*), or HLA-DQ2α3β (*D*). Controls are similar to those presented in Fig. 2. Data shown are the average ± SEM from between 6 and 12 independent experiments. *, $p < 0.05$, **, $p < 0.01$.

Table I. *Summary of functional characteristics for the SpeC mutants*[a]

SpeC Protein	LG-2 Cell Aggregation[b]	Activation of Vβ2.1$^+$ T Cells[c]			
		LG-2	BLS-DR1	BLS-DR4	BLS-DQ2α3β
Wild type	+	+	+	+	+
Y15A	+	−	−	−	−
F31A	+	+	+	+	+
T33A	+	+	+	(−)	+
T34A	+	+	+	+	(−)
H35A	+	+	+	+	(−)
T36A	+	(−)	(−)	(−)	+
N38A	+	+	(−)	+	+
Y50A	−	−	−	−	(−)
S52A	+	+	+	+	+
E54A	+	+	+	+	(−)
S56A	+	+	+	+	+
Y57A	+	+	+	+	+
E58A	+	+	+	+	+
Y76A	−	(−)	−	−	(−)
I77A	+	(−)	−	−	+
S80A	+	+	+	+	+
Y85A	+	(−)	−	−	+
Y87A	−	−	−	−	−
S182A	+	+	+	+	+
D183A	+	(−)	−	−	+
K189A	+	+	+	+	+
D203A	−	−	−	−	−
Y87A/D203A	ND[d]	−	−	−	−

[a] Data are summarized as follows: +, no significant deviation from the wild-type SpeC protein; (−), activity was still present but significantly reduced from that of wild type; −, no significant activity in comparison with the control condition.

[b] Aggregation of the LG-2 B cell line was scored at the 6-h time point as the number of cells in clumps as a percentage of the total number of cells in the field.

[c] Activation of the Vβ2.1$^+$ Jurkat T cells using different sources of MHC II as indicated.

[d] Not determined.

In the absence of crystallographic information, the precise intermolecular contacts between the β-barrel domain of SpeC and the α-chain of MHC II are unknown. Therefore, we generated a three-dimensional model of how SpeC would potentially engage MHCα (Fig. 5*D*). Despite low sequence identity, the N-terminal domain of SpeC is structurally more similar to TSST-1 (47) than to the group II and III SAgs; however, superposition of the SpeC-Vβ2.1 complex (13) onto the TSST-1-HLA-DR1 complex (3) generates major steric clashes between the CDR 3 loops of both TCRα and TCRβ with the MHC β1 domain and, thus, a similar orientation of SpeC and TSST-1 with MHC II is unlikely. Superposition of SpeC-Vβ2.1 complex onto the SEC_3-HLA-DR1 complex, with minor alterations, produced a model with a number of features that explain our mutagenesis data. SpeC (in complex with Vβ2.1) was first superimposed onto the crystal structures of SEC_3 in complex with HLA-DR1 (4). Because the molecular surface of SpeC important for engaging MHCα is significantly different from those of SAgs with structurally characterized MHCα interactions (discussed below), the complex was further manually docked based on our mutagenesis and functional data. Finally, the high-affinity, zinc-dependent MHC II interaction (6) and a human TCR α-chain (53) were superimposed onto the SpeC-Vβ2.1 complex. In this model, only minor steric clashes were found to occur between the TCR α-chain CDR2 and the MHC II β-chain (Fig. 5*D*).

Fig. 5*E* shows a ribbon diagram of residues from Ile^8 to Asn^{78} of the α-1 domain of HLA-DR1 (DRA*0101). Side chains of DRA*0101 that make known intermolecular contacts with SEA, SEB, or SEC_3 (2, 4, 8) are shown and labeled. Conserved side chains are colored gray, and side chains that differ between DRA*0101 and DQA1*0501 are colored magenta and orange, respectively. By combining our functional data (Fig. 5*B*) and the proposed model (Fig. 5*D*), the critical mutations in SpeC important for the engagement of HLA-DR4 form a near continuous surface

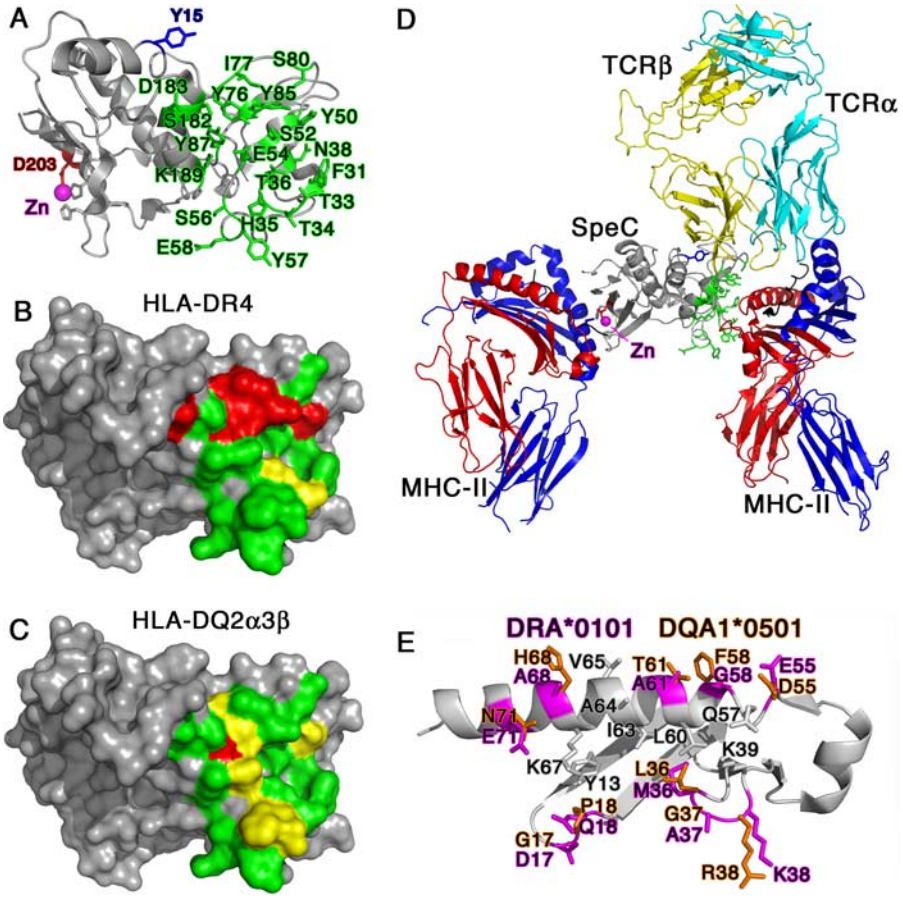

FIGURE 5. The SpeC functional epitope for engagement of MHC II and structural models of the SpeC-mediated T cell activation complex. *A*, Ribbon diagram of SpeC showing relevant amino acid side chains including the locations of all mutated residues within the putative low-affinity MHCα binding interface (green), as well as the location of the control mutation at position Tyr^{15} within the TCR Vβ interface (blue) and at position Asp^{203} within the high-affinity MHCβ interface (red). *B* and *C*, Surface representations of the SpeC functional epitope for interaction with HLA-DR4 (*B*) and HLA-DQ2α3β (*C*) in the same orientation as in *A*. Mutated residues that were functionally critical for the interaction are shown in red, residues that demonstrated minor to moderate reductions in activity are shown in yellow, and residues with little to no effect on the interaction are shown in green. *D*, Modeled SpeC-mediated activation complex generated as described in *Materials and Methods*. *E*, Ribbon diagram of MHCα showing the predicted "foot-print" of SpeC. Side chains of all amino acids that form intermolecular contacts with SEA, SEB, or SEC_3 are shown, and those differing between DRA*0101 (magenta) and DQA1*0501 (orange) are indicated.

predicted to make contacts within the first α-helix (MHCα residues αAsp^{55} to αAla^{68}) and αLys^{39} of MHCα, whereas the intermediate SpeC mutations likely form contacts with the loop between the β1 and β2 strands near the MHCα residue αGln^{18} (Fig. 5*E*).

Our model also predicts that the majority of residues important for the engagement of HLA-DQ2α3β form a thin but continuous surface, starting at SpeC Tyr^{76} and ending at Thr^{34} (Figs. 5, *A* and *C*). The one critical residue from the HLA-DQ2α3β analysis, Tyr^{87}, which is also critical for engaging the HLA-DR isoforms, likely hydrogen bonds with the side chain from the invariant MHCα residue Lys^{39}. Our model also predicts that the lower portions of the SpeC-HLA-DQ2α3β interface would fit in a pocked formed between the MHCα β1-β2 and β3-β4 loops, potentially interacting with αPro^{18}/αSer^{19} and αLeu^{36}/αGly^{37}/αArg^{38} (Fig. 5*E*).

Discussion

Bacterial SAgs represent a unique class of microbial toxins that have evolved to target the TCR and MHC II. The collective family of bacterial SAgs now vastly exceeds those that have been characterized with their TCR and MHC ligands on a structural level, and although there exists a high degree of structural homology between these SAgs, dramatically distinct molecular architectures of the SAg-mediated T cell signaling complexes can be formed (25).

In terms of MHCα engagement by bacterial SAgs, nearly all of the structural and functional analyses have been conducted with SAgs belonging to the group I (TSST-1), group II (SEB, SEC3, SpeA, and SSA (streptococcal superantigen)), and group III (SEA and SED) evolutionary lineages (2–4, 28, 30, 31, 56–58). In each case, the SAg N-terminal β-barrel domain is responsible for binding MHCα in a relatively low-affinity manner. Of these SAgs, TSST-1 represents an outlier where it binds predominantly to the MHC α-subunit, but it also extends over the antigenic peptide and makes contacts with the MHC β-subunit (3). Of the group II (SEB and SEC_3) and III (SEA) SAgs that have been structurally characterized in complex with MHCα, each have similar "footprints" on MHCα, although SEA is rotated slightly away from HLA-DR1, presenting a smaller contact surface (8) with a reduced affinity (31, 59). Not surprisingly, the molecular surfaces of the β-barrel domains in group II and group III SAgs, which also includes SpeA and SSA (60, 61), are generally similar.

MHC II α-chains are much more conserved than β-chains, and HLA-DR α-chains are conserved to one known isoform (DRA*0101). Thus, in our experiments using HLA-DR1 and HLA-DR4, the α-chain is constant. Although the crystal structure of SpeC in complex with MHCα has not been solved, SpeC has been crystallized through the high-affinity MHCβ interaction with HLA-DR2a (DRA*0101/DRB5*0101) (6). In this case, the $SpeC_{H35A}$ mutant was used because the wild-type SpeC did not crystallize with HLA-DR2a, implying that an alternative interface was located at this site. Of the residues from DRB5*0101 that contact SpeC, each are conserved between DRB1*0101 and DRB1*0401 with one notable difference (DRB5*0101 Asp^{71} is a Gln in both DRB1 isoforms) (6). Thus, the contacts between SpeC and MHCβ from HLA-DR1 and HLA-DR4 are assumed to be identical. However, we did see a roughly 2-fold difference in potency exhibited by the BLS lines expressing HLA-DR4 or HLA-DR1 (Fig. 4, *B* and *C*). These differences could be explained, in part, by the different peptides displayed in these MHC II molecules

(27), as the peptide binding pockets are not identical. These variations could also be explained by potential differences in MHC II expression between transfectants, although no apparent difference in median fluorescence intensity was observed by flow cytometry when these cells were stained for HLA-DR expression (data not shown). Experiments conducted with HLA-DQ2α3β, as expected (42), were functionally much less efficient than those conducted with either HLA-DR molecule (Fig. 4*A*). Again from the SpeC-HLA-DR2a complex, most of the residues predicted to engage DRB1*0101 and DRB1*0401 are conserved in DQB1*0302, including all those that form hydrogen bonds with SpeC (βThr^{21}, βAsp^{76}, βThr^{77}, βArg^{80}, and βHis^{81}) (6). One exception includes position βGly^{84} in DRB1*0101 and DRB1*0401 (βGln^{84} in DQB1*0302), which forms van der Waals contacts. Based on the model in Fig. 5*D*, the predicted SpeC "footprint" on MHCα contains a number of altered residues. These are illustrated in Fig. 5*E*, where conserved MHCα side-chains are colored gray, DRA*0101-specific residues are colored magenta, and DQA1*0501-specific residues are colored orange. Thus, within our experimental system for the functional interaction of SpeC with the different MHC II isoforms, minor differences in MHCβ-chain residues, or different antigenic peptides (27), may potentially influence the activation experiments. However, due to the large number of altered residues between DRA*0101 and DQA1*0501 (Fig. 5*E*), we believe that the major functional differences observed are most likely due to different α-chain contacts.

When comparing SpeC on a structural level with other SAgs, one strikingly common feature within the β-barrel domain of group II, group III, and group IV SAgs is the "polar pocket" region, corresponding to SpeC residues Glu^{54}, Tyr^{76}, and Tyr^{87}. In group II and group III SAgs, this region engages the invariant αLys^{39} residue. SpeC Tyr^{87} was of critical importance in all of our functional assays, including the engagement of both HLA-DR and HLA-DQ isoforms. The SpeC$_{Y76A}$ mutation, however, was critical for interaction with HLA-DR but showed an intermediate phenotype for HLA-DQ2α3β, whereas SpeC$_{E54A}$ did not produce a phenotype for either HLA-DR molecule but showed an intermediate phenotype for HLA-DQ2α3β. Taken together, the mutagenesis data within this region indicate that SpeC residues Tyr^{76} and Tyr^{87} likely form hydrogen bonds with the αLys^{39} side chain, analogous with SEC$_3$. The observation that SpeC$_{E54A}$ did not produce a more drastic phenotype was surprising in that the equivalent residues SEA Asp^{70}, SEB Glu^{67} and SEC$_3$ Glu^{67} each form a key salt bridge with αLys^{39}. This indicates that SpeC Glu^{54} does not form an equivalent salt bridge with αLys^{39}. Although conserved as either an Asp or Glu in most group IV SAgs, the group IV SAg *Streptococcus dysgalactiae*-derived mitogen contains an Asn at this position, a residue predicted to disable a salt bridge with αLys^{39} (62). Thus, this residue may be largely dispensable for group IV SAg function, at least for engagement with HLA-DR. Comparing the HLA-SEA and HLA-SEC$_3$ complexes, SEA binding to MHCα is rotated slightly away relative to SEC$_3$. This rotation allows for the salt bridge between SEA Asp^{70} and αLys^{39}, but SEA Tyr^{92} and SEA Tyr^{108} (corresponding to SpeC Tyr^{76} and SpeC Tyr^{87}) are displaced away and are too far to form hydrogen bonds with αLys^{39} (8). Our data predict the reverse scenario with SpeC, where this SAg binds more distal to the antigenic peptide in HLA-DR, precluding the salt bridge and explaining why Glu^{54} is not critical. With HLA-DQ2α3β, SpeC residues Glu^{54}, Tyr^{76}, and Tyr^{87} were all important, indicating that with this isoform SpeC likely engages in a slightly "higher" position more analogous with SEC$_3$.

Aside from the polar pocket region, the remaining surface of the SpeC β-barrel predicted to engage MHCα is drastically different compared with group II and group III SAgs. A flexible loop region found in the SEs termed the "cysteine loop," which is located between the β4 and β5 strands (residues Cys^{93} to Cys^{110} in SEC$_3$), is unique to group II and group III SAgs. This region corresponds to SpeC residues Asn^{79} through Gly^{83}. In group II and group III SAgs, the proximal region of the loop extends away from the SAg surface making a number of contacts with MHCα (e.g., SEC$_3$ residues Asn^{92}, Tyr^{94}, and Ser^{96}) (4). In SpeC, the β4-β5 region is much shorter, and this results in a concave surface on SpeC where the majority of the residues critical for engagement of HLA-DR map (SpeC residues Tyr^{50}, Tyr^{76}, Ile^{77}, and Tyr^{85}) (Fig. 5*B*). Our model predicts that the α-helix from the MHC α-1 domain would fit into this groove (Fig. 5*D*), thus explaining this functional "hot spot". Within this region, SpeC$_{Y50A}$ resulted in a critical phenotype when presented by LG-2 cells or cells expressing either HLA-DR1 or HLA-DR4. However, an intermediate phenotype was shown for the HLA-DQ2α3β cell line. SpeC$_{I77A}$ and SpeC$_{Y85A}$ produced a similar phenotype, although reduced activity did not reach statistical significance for the HLA-DQ2α3β cell line. Based on our model, these three residues likely engage the α1 domain, near to positions αAla^{61} and αAla^{68} found in DRA*0101 (Fig. 5*E*). These two residues are αThr^{61} and αHis^{68} in DQA1*0501 (Fig. 5*E*), which may partially occlude insertion of the α1 domain onto the surface of SpeC, and this is consistent with the polar pocket mutations where the SpeC β4-β5 loop would be pushed laterally, forcing SpeC to bind "higher" on the HLA-DQ2α3β surface. This isoform variation in MHCα may represent a key mechanism that results in allelic discrimination between HLA-DQ alleles, from HLA-DR, at least for SpeC. One of the most dramatic differences between the HLA-DR and HLA-DQ isoforms resulted from the mutation at SpeC Asp^{183}. The mutation appears to be an outlier from the other mutations and may require a water molecule to bridge the intermolecular contacts with MHCα. The most likely contact in DRA*0101 would be αGlu^{55}, because DQA1*0501 contains a shorter side chain Asp^{55} that may prevent intermolecular contacts (Fig. 5*E*). Lastly, for both HLA-DR isoforms SpeC$_{S80A}$ consistently produced a mildly but significantly increased activation phenotype compared with wild-type SpeC. The reason for this is unknown, but from the Vβ2.1-SpeC crystal structure SpeC Asn^{79} formed hydrogen bonds with the main chain of the Vβ2.1 CDR3 loop, and the SpeC$_{S80A}$ mutant may alter these contacts. This would be consistent with HLA-DQ2α3β, where this region of the loop would be more distal to the Vβ CDR3 loop, and the SpeC$_{S80A}$ mutant did not show an increase in activity.

The other notable difference between group II, group III, and group IV SAgs within the β-barrel domain is a loop located between the β1–β2 sheets in SEs termed the "hydrophobic ridge". Compared with SpeC, this ridge is extended by one additional amino acid in SEA, SEB, and SEC$_3$. This results in an altered orientation, such that there are no similarly positioned residues for SpeC residues Phe^{31}, Ser^{32}, and Thr^{33}. However, within the group IV subclass, this loop is structurally conserved (e.g., SpeC, SpeG, SpeJ, and SMEZ (streptococcal mitogenic exotoxin Z)). This region in SEC$_3$ in functionally important because a series of hydrophobic loop variants, generated by random mutagenesis coupled with phage display to select for affinity matured variants, resulted in variants with nearly 60-fold stronger binding affinities for HLA-DR1 (4). Within this region in SpeC, mutations important for engagement with HLA-DR4 that were not important for engagement with HLA-DQ2α3β were at SpeC positions Thr^{33}and Thr^{36}. Thr^{33} could potentially interact directly with αGln18 (Fig. 5*E*), whereas Thr^{36} forms a concave surface on the SpeC molecular surface (Fig. 5*B*). It is difficult to envision from the model any direct interactions between Thr^{36}and MHCα. The Oγ1 atom on Thr^{36} forms a

hydrogen bond with Thr[33] Oγ1, and this interaction may be important for the orientation of Thr[33] to make productive contacts with αGln[18]. This would be consistent with the HLA-DQ2α3β interaction, where neither mutation produced a phenotype. Mutation at this position produced an intermediate phenotype for HLA-DR4, but not for HLA-DR1 or HLA-DQ2α3β. The opposite phenotype was seen for the SpeC Asn[38] mutation, where there was no difference for activation by HLA-DR4 while there was a minor defect for HLA-DR1. The reasons for these minor differences are not readily apparent, as the α-chains for HLA-DR1 and HLA-DR4 are identical. It is formally possible that β-chain polymorphisms influence the α-chain conformation within this region or that altered peptide-SAg interactions between the two HLA-DR isoforms indirectly influence the α-chain-SpeC interaction. Thr[34] is not a conserved residue among SAgs characterized to engage MHCα, and the $SpeC_{T34A}$ mutation displayed only a minor reduction in activation for HLA-DQ2α3β. SpeC His[35] however, represents a highly conserved residue that is also found at this position in SSA, SpeA, SEA, and SEC3 (in SEB it is Phe[47]). Our data indicate that despite the conservation of this residue in other SAgs, with SpeC it played no role for the engagement of HLA-DR isoforms but did show an intermediate phenotype with HLA-DQ. The most likely explanation for this is that αGly[37] present in HLA-DQ alleles (αAla[37] in DRA*0101) (Fig. 5*E*) allows for a more flexible loop in this region that could accommodate DQA1*0501 main chain interactions with the SpeC His[35] side chain.

SpeC belongs to the SAg group IV, an evolutionary branch that contains only streptococcal SAgs, and group IV SAgs have been poorly characterized with respect to MHCα engagement. Our data have revealed a functional epitope within the SpeC β-barrel domain that is critical for engagement of HLA-DR and indicates that SpeC, similarly as group I, group II, and group III Sags, possesses a low-affinity MHC II binding interface that is required for the activation of T cells. Our data also predict that polymorphisms within the α-1 domain of MHCα may be primarily responsible for the weak activity associated with SpeC when presented by HLA-DQ isoforms and that in such cases SpeC likely engages in an inefficient and slightly altered orientation. Although the β-barrel domain of group IV SAgs is considerably different from those of group II and group III SAgs, our functional experiments indicate that the polar pocket region, which is conserved in group II, group III, and group IV SAgs, may represent a new rational target for broad spectrum inhibitors of bacterial SAgs.

Disclosures

The authors have no financial conflict of interest.

References

1. Dessen, A., C. M. Lawrence, S. Cupo, D. M. Zaller, and D. C. Wiley. 1997. X-ray crystal structure of HLA-DR4 (DRA*0101, DRB1*0401) complexed with a peptide from human collagen II. *Immunity* 7: 473–481.
2. Jardetzky, T. S., J. H. Brown, J. C. Gorga, L. J. Stern, R. G. Urban, Y. I. Chi, C. Stauffacher, J. L. Strominger, and D. C. Wiley. 1994. Three-dimensional structure of a human class II histocompatibility molecule complexed with superantigen. *Nature* 368: 711–718.
3. Kim, J., R. G. Urban, J. L. Strominger, and D. C. Wiley. 1994. Toxic shock syndrome toxin-1 complexed with a class II major histocompatibility molecule HLA-DR1. *Science* 266: 1870–1874.
4. Sundberg, E. J., P. S. Andersen, P. M. Schlievert, K. Karjalainen, and R. A. Mariuzza. 2003. Structural, energetic, and functional analysis of a protein-protein interface at distinct stages of affinity maturation. *Structure* 11: 1151–1161.
5. Fernandez, M. M., R. Guan, C. P. Swaminathan, E. L. Malchiodi, and R. A. Mariuzza. 2006. Crystal structure of staphylococcal enterotoxin I (SEI) in complex with a human major histocompatibility complex class II molecule. *J. Biol. Chem.* 281: 25356–25364.
6. Li, Y., H. Li, N. Dimasi, J. K. McCormick, R. Martin, P. Schuck, P. M. Schlievert, and R. A. Mariuzza. 2001. Crystal structure of a superantigen bound to the high-affinity, zinc- dependent site on MHC class II. *Immunity* 14: 93–104.
7. Petersson, K., M. Hakansson, H. Nilsson, G. Forsberg, L. A. Svensson, A. Liljas, and B. Walse. 2001. Crystal structure of a superantigen bound to MHC class II displays zinc and peptide dependence. *EMBO J.* 20: 3306–3312.
8. Petersson, K., M. Thunnissen, G. Forsberg, and B. Walse. 2002. Crystal structure of a SEA variant in complex with MHC class II reveals the ability of SEA to crosslink MHC molecules. *Structure* 10: 1619–1626.
9. Cho, S., C. P. Swaminathan, J. Yang, M. C. Kerzic, R. Guan, M. C. Kieke, D. M. Kranz, R. A. Mariuzza, and E. J. Sundberg. 2005. Structural basis of affinity maturation and intramolecular cooperativity in a protein-protein interaction. *Structure* 13: 1775–1787.
10. Fields, B. A., E. L. Malchiodi, H. Li, X. Ysern, C. V. Stauffacher, P. M. Schlievert, K. Karjalainen, and R. A. Mariuzza. 1996. Crystal structure of a T-cell receptor β-chain complexed with a superantigen. *Nature* 384: 188–192.
11. Li, H., A. Llera, D. Tsuchiya, L. Leder, X. Ysern, P. M. Schlievert, K. Karjalainen, and R. A. Mariuzza. 1998. Three-dimensional structure of the complex between a T cell receptor β chain and the superantigen staphylococcal enterotoxin B. *Immunity* 9: 807–816.
12. Moza, B., A. K. Varma, R. A. Buonpane, P. Zhu, C. A. Herfst, M. J. Nicholson, A.-K. Wilbuer, K. W. Wucherpfennig, J. K. McCormick, D. M. Kranz, and E. J. Sundberg. 2007. Structural basis of T cell specificity and activation by the bacterial superantigen toxic shock syndrome toxin-1. *EMBO J.* 26: 1187–1197.
13. Sundberg, E. J., H. Li, A. S. Llera, J. K. McCormick, J. Tormo, P. M. Schlievert, K. Karjalainen, and R. A. Mariuzza. 2002. Structures of two streptococcal superantigens bound to TCR β chains reveal diversity in the architecture of T cell signaling complexes. *Structure* 10: 687–699.
14. Yang, J., C. P. Swaminathan, Y. Huang, R. Guan, S. Cho, M. C. Kieke, D. M. Kranz, R. A. Mariuzza, and E. J. Sundberg. 2003. Dissecting cooperative and additive binding energetics in the affinity maturation pathway of a protein-protein interface. *J. Biol. Chem.* 278: 50412–50421.
15. Günther, S., A. K. Varma, B. Moza, K. J. Kasper, A. W. Wyatt, P. Zhu, A. K. Rahman, Y. Li, R. A. Mariuzza, J. K. McCormick, and E. J. Sundberg. 2007. A novel loop domain in superantigens extends their T cell receptor recognition site. *J. Mol. Biol.* 371: 210–221.
16. Marrack, P., and J. Kappler. 1990. The staphylococcal enterotoxins and their relatives. *Science* 248: 705–711.
17. Faulkner, L., A. Cooper, C. Fantino, D. M. Altmann, and S. Sriskandan. 2005. The mechanism of superantigen-mediated toxic shock: not a simple Th1 cytokine storm. *J. Immunol.* 175: 6870–6877.
18. McCormick, J. K., J. M. Yarwood, and P. M. Schlievert. 2001. Toxic shock syndrome and bacterial superantigens: an update. *Annu. Rev. Microbiol.* 55: 77–104.
19. Bachert, C., N. Zhang, J. Patou, T. van Zele, and P. Gevaert. 2008. Role of staphylococcal superantigens in upper airway disease. *Curr. Opin. Allergy Clin. Immunol.* 8: 34–38.
20. Matsubara, K., and T. Fukaya. 2007. The role of superantigens of group A *Streptococcus* and *Staphylococcus aureus* in Kawasaki disease. *Curr. Opin. Infect. Dis.* 20: 298–303.
21. Sawitzke, A. D., H. H. Mu, and B. C. Cole. 1999. Superantigens and autoimmune disease: are they involved? *Curr. Opin. Infect. Dis.* 12: 213–219.
22. Sicat, J., N. Sutkowski, and B. T. Huber. 2005. Expression of human endogenous retrovirus HERV-K18 superantigen is elevated in juvenile rheumatoid arthritis. *J. Rheumatol.* 32: 1821–1831.
23. Proft, T., and J. D. Fraser. 2003. Bacterial superantigens. *Clin. Exp. Immunol.* 133: 299–306.
24. Brouillard, J. N., S. Gunther, A. K. Varma, I. Gryski, C. A. Herfst, A. K. Rahman, D. Y. Leung, P. M. Schlievert, J. Madrenas, E. J. Sundberg, and J. K. McCormick. 2007. Crystal structure of the streptococcal superantigen SpeI and functional role of a novel loop domain in T cell activation by group V superantigens. *J. Mol. Biol.* 367: 925–934.
25. Sundberg, E. J., L. Deng, and R. A. Mariuzza. 2007. TCR recognition of peptide/MHC class II complexes and superantigens. *Semin. Immunol.* 19: 262–271.
26. Li, H., A. Llera, E. L. Malchiodi, and R. A. Mariuzza. 1999. The structural basis of T cell activation by superantigens. *Annu. Rev. Immunol.* 17: 435–466.
27. Wen, R., G. A. Cole, S. Surman, M. A. Blackman, and D. L. Woodland. 1996. Major histocompatibility complex class II-associated peptides control the presentation of bacterial superantigens to T cells. *J. Exp. Med.* 183: 1083–1092.
28. Hudson, K. R., R. E. Tiedemann, R. G. Urban, S. C. Lowe, J. L. Strominger, and J. D. Fraser. 1995. Staphylococcal enterotoxin A has two cooperative binding sites on major histocompatibility complex class II. *J. Exp. Med.* 182: 711–720.
29. Tripp, T. J., J. K. McCormick, J. M. Webb, and P. M. Schlievert. 2003. The zinc-dependent major histocompatibility complex class II binding site of streptococcal pyrogenic exotoxin C is critical for maximal superantigen function and toxic activity. *Infect. Immun.* 71: 1548–1550.
30. Al-Daccak, R., K. Mehindate, F. Damdoumi, P. Etongue-Mayer, H. Nilsson, P. Antonsson, M. Sundstrom, M. Dohlsten, R. P. Sekaly, and W. Mourad. 1998. Staphylococcal enterotoxin D is a promiscuous superantigen offering multiple modes of interactions with the MHC class II receptors. *J. Immunol.* 160: 225–232.
31. Abrahmsen, L., M. Dohlsten, S. Segren, P. Bjork, E. Jonsson, and T. Kalland. 1995. Characterization of two distinct MHC class II binding sites in the superantigen staphylococcal enterotoxin A. *EMBO J.* 14: 2978–2986.
32. Thibodeau, J., M. Dohlsten, I. Cloutier, P. M. Lavoie, P. Bjork, F. Michel, C. Leveille, W. Mourad, T. Kalland, and R. P. Sekaly. 1997. Molecular characterization and role in T cell activation of staphylococcal enterotoxin A binding to the HLA-DR α-chain. *J. Immunol.* 158: 3698–3704.

33. Dowd, J. E., R. W. Karr, and D. R. Karp. 1996. Functional activity of staphylococcal enterotoxin A requires interactions with both the α and β chains of HLA-DR. *Mol. Immunol.* 33: 1267–1274.
34. Newton, D. W., M. Dohlsten, C. Olsson, S. Segren, K. E. Lundin, P. A. Lando, T. Kalland, and M. Kotb. 1996. Mutations in the MHC class II binding domains of staphylococcal enterotoxin A differentially affect T cell receptor Vβ specificity. *J. Immunol.* 157: 3988–3994.
35. Tiedemann, R. E., and J. D. Fraser. 1996. Cross-linking of MHC class II molecules by staphylococcal enterotoxin A is essential for antigen-presenting cell and T cell activation. *J. Immunol.* 157: 3958–3966.
36. Tiedemann, R. E., R. J. Urban, J. L. Strominger, and J. D. Fraser. 1995. Isolation of HLA-DR1. (staphylococcal enterotoxin A)2 trimers in solution. *Proc. Natl. Acad. Sci. USA* 92: 12156–12159.
37. Kansal, R. G., V. Nizet, A. Jeng, W. J. Chuang, and M. Kotb. 2003. Selective modulation of superantigen-induced responses by streptococcal cysteine protease. *J. Infect. Dis.* 187: 398–407.
38. Kotb, M., A. Norrby-Teglund, A. McGeer, H. El-Sherbini, M. T. Dorak, A. Khurshid, K. Green, J. Peeples, J. Wade, G. Thomson, et al. 2002. An immunogenetic and molecular basis for differences in outcomes of invasive group A streptococcal infections. *Nat. Med.* 8: 1398–1404.
39. Nooh, M. M., N. El-Gengehi, R. Kansal, C. S. David, and M. Kotb. 2007. HLA transgenic mice provide evidence for a direct and dominant role of HLA class II variation in modulating the severity of streptococcal sepsis. *J. Immunol.* 178: 3076–3083.
40. Sriskandan, S., M. Unnikrishnan, T. Krausz, H. Dewchand, S. Van Noorden, J. Cohen, and D. M. Altmann. 2001. Enhanced susceptibility to superantigen-associated streptococcal sepsis in human leukocyte antigen-DQ transgenic mice. *J. Infect. Dis.* 184: 166–173.
41. Llewelyn, M., S. Sriskandan, M. Peakman, D. R. Ambrozak, D. C. Douek, W. W. Kwok, J. Cohen, and D. M. Altmann. 2004. HLA class II polymorphisms determine responses to bacterial superantigens. *J. Immunol.* 172: 1719–1726.
42. Norrby-Teglund, A., G. T. Nepom, and M. Kotb. 2002. Differential presentation of group A streptococcal superantigens by HLA class II DQ and DR alleles. *Eur. J. Immunol.* 32: 2570–2577.
43. DaSilva, L., B. C. Welcher, R. G. Ulrich, M. J. Aman, C. S. David, and S. Bavari. 2002. Humanlike immune response of human leukocyte antigen-DR3 transgenic mice to staphylococcal enterotoxins: a novel model for superantigen vaccines. *J. Infect. Dis.* 185: 1754–1760.
44. Welcher, B. C., J. H. Carra, L. DaSilva, J. Hanson, C. S. David, M. J. Aman, and S. Bavari. 2002. Lethal shock induced by streptococcal pyrogenic exotoxin A in mice transgenic for human leukocyte antigen-DQ8 and human CD4 receptors: implications for development of vaccines and therapeutics. *J. Infect. Dis.* 186: 501–510.
45. Sambrook, J., and D. W. Russell. 2001. *Molecular Cloning: A Laboratory Manual.* Cold Spring Harbor Laboratory Press, Cold Spring Harbor, NY.
46. Li, P. L., R. E. Tiedemann, S. L. Moffat, and J. D. Fraser. 1997. The superantigen streptococcal pyrogenic exotoxin C (SPE-C) exhibits a novel mode of action. *J. Exp. Med.* 186: 375–383.
47. Roussel, A., B. F. Anderson, H. M. Baker, J. D. Fraser, and E. N. Baker. 1997. Crystal structure of the streptococcal superantigen SPE-C: dimerization and zinc binding suggest a novel mode of interaction with MHC class II molecules. *Nat. Struct. Biol.* 4: 635–643.
48. Swietnicki, W., A. M. Barnie, B. K. Dyas, and R. G. Ulrich. 2003. Zinc binding and dimerization of *Streptococcus pyogenes* pyrogenic exotoxin C are not essential for T-cell stimulation. *J. Biol. Chem.* 278: 9885–9895.
49. Rahman, A. K., C. A. Herfst, B. Moza, S. R. Shames, L. A. Chau, C. Bueno, J. Madrenas, E. J. Sundberg, and J. K. McCormick. 2006. Molecular basis of TCR selectivity, cross-reactivity, and allelic discrimination by a bacterial superantigen: integrative functional and energetic mapping of the SpeC-Vβ2.1 molecular interface. *J. Immunol.* 177: 8595–8603.
50. Kapust, R. B., J. Tozser, J. D. Fox, D. E. Anderson, S. Cherry, T. D. Copeland, and D. S. Waugh. 2001. Tobacco etch virus protease: mechanism of autolysis and rational design of stable mutants with wild-type catalytic proficiency. *Protein Eng.* 14: 993–1000.
51. Fraser, J. D., R. G. Urban, J. L. Strominger, and H. Robinson. 1992. Zinc regulates the function of two superantigens. *Proc. Natl. Acad. Sci. USA* 89: 5507–5511.
52. Gorga, J. C., V. Horejsi, D. R. Johnson, R. Raghupathy, and J. L. Strominger. 1987. Purification and characterization of class II histocompatibility antigens from a homozygous human B cell line. *J. Biol. Chem.* 262: 16087–16094.
53. Hennecke, J., A. Carfi, and D. C. Wiley. 2000. Structure of a covalently stabilized complex of a human $\alpha\beta$ T-cell receptor, influenza HA peptide and MHC class II molecule, HLA-DR1. *EMBO J.* 19: 5611–5624.
54. Bueno, C., C. D. Lemke, G. Criado, M. L. Baroja, S. S. Ferguson, A. K. Rahman, C. D. Tsoukas, J. K. McCormick, and J. Madrenas. 2006. Bacterial superantigens bypass Lck-dependent T cell receptor signaling by activating a Gα11-dependent, PLC-β-mediated pathway. *Immunity* 25: 67–78.
55. Nekrep, N., J. D. Fontes, M. Geyer, and B. M. Peterlin. 2003. When the lymphocyte loses its clothes. *Immunity* 18: 453–457.
56. Ulrich, R. G., S. Bavari, and M. A. Olson. 1995. Staphylococcal enterotoxins A and B share a common structural motif for binding class II major histocompatibility complex molecules. *Nat. Struct. Biol.* 2: 554–560.
57. Kappler, J. W., A. Herman, J. Clements, and P. Marrack. 1992. Mutations defining functional regions of the superantigen staphylococcal enterotoxin B. *J. Exp. Med.* 175: 387–396.
58. Kline, J. B., and C. M. Collins. 1996. Analysis of the superantigenic activity of mutant and allelic forms of streptococcal pyrogenic exotoxin A. *Infect. Immun.* 64: 861–869.
59. Mollick, J. A., M. Chintagumpala, R. G. Cook, and R. R. Rich. 1991. Staphylococcal exotoxin activation of T cells: role of exotoxin-MHC class II binding affinity and class II isotype. *J. Immunol.* 146: 463–468.
60. Papageorgiou, A. C., C. M. Collins, D. M. Gutman, J. B. Kline, S. M. O'Brien, H. S. Tranter, and K. R. Acharya. 1999. Structural basis for the recognition of superantigen streptococcal pyrogenic exotoxin A (SpeA1) by MHC class II molecules and T-cell receptors. *EMBO J.* 18: 9–21.
61. Sundberg, E., and T. S. Jardetzky. 1999. Structural basis for HLA-DQ binding by the streptococcal superantigen SSA. *Nat. Struct. Biol.* 6: 123–129.
62. Saarinen, S., H. Kato, T. Uchiyama, T. Miyoshi-Akiyama, and A. C. Papageorgiou. 2007. Crystal structure of *Streptococcus dysgalactiae*-derived mitogen reveals a zinc-binding site and alterations in TcR binding. *J. Mol. Biol.* 373: 1089–1097.
63. Karp, D. R., and E. O. Long. 1992. Identification of HLA-DR1 β chain residues critical for binding staphylococcal enterotoxins A and E. *J. Exp. Med.* 175: 415–424.